pISSN 1598-2998, eISSN 2005-9256

Cancer Res Treat. 2020;52(4):1084-1102 https://doi.org/10.4143/crt.2020.093

Original Article Open Access

β1,4-Galactosyltransferase V Modulates Breast Cancer Stem Cells through Wnt/β-catenin Signaling Pathway

Wei Tang, BD[1]
Meng Li, MD[1]
Xin Qi, PhD[1]
Jing Li, PhD[1,2,3]

[1]*Key Laboratory of Marine Drugs, Chinese Ministry of Education, School of Medicine and Pharmacy, Ocean University of China, Qingdao,* [2]*Laboratory for Marine Drugs and Bioproducts of Qingdao National Laboratory for Marine Science and Technology, Qingdao,* [3]*Open Studio for Druggability Research of Marine Natural Products, Pilot National Laboratory for Marine Science and Technology (Qingdao), Qingdao, China*

Correspondence: Jing Li, PhD
Key Laboratory of Marine Drugs, Chinese Ministry of Education, School of Medicine and Pharmacy, Ocean University of China, Yushan Road No. 5, Qingdao 266003, China
Tel: 81-0532-82031980
Fax: 81-0532-82031980
E-mail: lijing_ouc@ouc.edu.cn

Received February 8, 2020
Accepted May 25, 2020
Published Online May 27, 2020

Purpose
Breast cancer stem cells (BCSCs) contribute to the initiation, development, and recurrence of breast carcinomas. β1,4-Galactosyltransferase V (B4GalT5), which catalyzes the addition of galactose to GlcNAcβ1-4Man of N-glycans, is involved in embryogenesis. However, its role in the modulation of BCSCs remains unknown.

Materials and Methods
The relationship between B4GalT5 and breast cancer stemness was investigated by online clinical databases and immunohistochemistry analysis. Mammosphere formation, fluorescence-activated cell sorting (FACS), and *in-vivo* assays were used to evaluate B4GalT5 expression in BCSCs and its effect on BCSCs. B4GalT5 regulation of Wnt/β-catenin signaling was examined by immunofluorescence and *Ricinus communis* agglutinin I pull-down assays. Cell surface biotinylation and FACS assays were performed to assess the association of cell surface B4GalT5 and BCSCs.

Results
B4GalT5, but not other B4GalTs, was highly correlated with BCSC markers and poor prognosis. B4GalT5 significantly increased the stem cell marker aldehyde dehydrogenase 1A1 (ALDH1A1) and promoted the production of $CD44^{+}CD24^{-/low}$ cells and the formation of mammospheres. Furthermore, B4GalT5 overexpression resulted in dramatic tumor growth *in vivo*. Mechanistically, B4GalT5 modified and protected Frizzled-1 from degradation via the lysosomal pathway, promoting Wnt/β-catenin signaling which was hyperactivated in BCSCs. B4GalT5, located on the surface of a small subset of breast carcinoma cells, was not responsible for the stemness of BCSCs.

Conclusion
B4GalT5 modulates the stemness of breast cancer through glycosylation modification to stabilize Frizzled-1 and activate Wnt/β-catenin signaling independent of its cell surface location. Our studies highlight a previously unknown role of B4GalT5 in regulating the stemness of breast cancer and provide a potential drug target for anticancer drug development.

Key words
β1,4-Galactosyltransferase V, Breast cancer stem cell, Cellular location, Frizzled-1, Glycosylation

Introduction

Breast cancer is one of the most common malignant cancers among women worldwide with more than 2 million new cases expected to be diagnosed and 600 thousand deaths in 2018 [1]. Although current treatments, to a certain extent, effectively reduce tumor bulk, many patients with breast cancer still experience recurrence, metastasis, and ultimately death.

Cancer stem cells (CSCs) are a small subset of poorly differentiated tumor cells within a tumor that show self-renewal and differentiation into heterogeneous lineages [2]. CSCs also account for chemo- and radioresistance, resulting in tumor recurrence and eventually metastasis due to the failure of current treatments [2]. Moreover, breast cancer stem cells (BCSCs) are regulated by several transcriptional factors

and signaling pathways, such as Nanog, Oct4, Notch pathway, and Wnt/β-catenin pathway [3]. Extensive evidence has shown that BCSCs are a crucial factor that contributes to the initiation, development, relapse, and chemoresistance of breast cancer.

A growing body of evidence supports aberrant glycosylation of cell surface receptors as a consequence of oncogenic transformation in different aspects of tumor progression, including proliferation, invasion, angiogenesis, and metastasis [4]. Within a tumor, altered glycosylation of proteins is frequently attributed to abnormal expression of glycosyltransferases [5]. Therefore, these enzymes are considered therapeutic targets, as aberrant glycans may be involved in promoting tumor progression and metastasis.

The β1,4-galactosyltransferase (B4GalT) family belongs to type II membrane-bound glycoproteins mainly located in the Golgi apparatus that exclusively transfer an active UDP-galactose in a β1,4 linkage to acceptor sugars [6]. There are currently seven members of the β4GalT gene family, B4Gal-T1-T7, which participate in the biosynthesis of different glycoconjugates and saccharide structures with slightly different substrate affinities and end products [6]. Specifically, B4GalT5 has been reported to catalyze the addition of galactose to GlcNAcβ1-4Man of glycans and functions as an important regulator in extraembryonic development [6]. Considerable research has revealed that extraembryonic development shares similarities with tumorigenesis in terms of biological behaviors (such as migration and invasion, gene expression and protein profiles, signaling pathways, and cell differentiation) [7], strongly suggesting that B4GalT5 may be involved in modulating the stemness of BCSCs. In this study, we demonstrated that B4GalT5 is upregulated in BCSCs to maintain the stemness of these cells by glycosylating the receptor Frizzled-1 and constantly activating Wnt/β-catenin signaling. Furthermore, we showed that B4GalT5 is located on the cell surface of a small subset of breast cancer cells, but cell surface localization did not play a decisive role in the stemness of BCSCs.

Materials and Methods

1. Reagents

Roswell Park Memorial Institute (RPMI) 1640 medium, minimum essential medium (MEM), Leibovitz's L-15 medium, Dulbecco's modified Eagle medium: nutrient mixture F-12 (DMEM/F-12), epidermal growth factor (EGF), basic fibroblast growth factor (bFGF), and B27 were purchased from Gibco (Grand Island, NY). Fetal bovine serum (FBS) and trypsin were purchased from Gibco-Invitrogen. Insulin and fluorescein isothiocyanate (FITC)-conjugated goat anti-rabbit antibody were purchased from Solarbio (Beijing, China). Antibodies to detect aldehyde dehydrogenase 1A1 (ALDH1A1), phosphorylated GSK3β (Ser 9), β-catenin, phosphorylated β-catenin (Ser 45), Erk, and His were products of Cell Signaling Technology (Boston, MA). SuperSignal West Femto Maximum Sensitivity Substrate, EZ-Link Sulfo-NHS-SS-Biotin, Pierce NeutrAvidin agarose, anti-B4GalT5, FITC-conjugated anti-CD44 and allophycocyanin (APC)-conjugated anti-CD24 antibodies were obtained from Thermo Scientific (Waltham, MA). Anti–Frizzled-1 and phycoerythrin (PE)-conjugated anti-His antibodies were purchased from R&D Systems (Minneapolis, MN). PE-conjugated anti–epithelial specific antigen antibody was purchased from Biolegend (San Diego, CA). The primary antibodies (β-actin and glyceraldehyde 3-phosphate dehydrogenase) and the secondary antibodies were purchased from HuaBio (Hangzhou, China). Horseradish peroxidase (HRP)-streptavidin, biotinylated *Ricinus communis* agglutinin I (RCA-I), and agarose-bound RCA-I were obtained from Vector Laboratories (Burlingame, CA). 3-(4,5-dimethyl-2-thiazolyl)-2,5-diphenyl-2-H-tetrazolium bromide (MTT) was purchased from Sigma-Aldrich (St. Louis, MO). The ALDEFLUOR Kit was purchased from Stem Cell Technologies (Vancouver, BC, Canada). The Mycoplasma PCR Detection Kit, DAPI, cell lysis buffer for western blot and immunoprecipitation (IP), phenylmethanesulfonylfluoride (PMSF), MG132, membrane and cytosol protein extraction kit and BCA Protein Assay Kit were purchased from Beyotime Institute of Biotechnology (Shanghai, China). B4GalT5 siRNA, NC siRNA, shB4GalT5 plasmid, and shNC plasmid were constructed by GenePharma (Shanghai, China). Triptolide with purity > 99% was obtained from Shanghai Institute of Materia Medica. Wnt 3β and leupeptin were obtained from the Laboratory of Molecular Medicine at Ocean University of China.

2. Tissue microarray

Tissue microarray (TMA; HBreD090CS01) was purchased from Shanghai Outdo Biotech Co., Ltd. (Shanghai, China). The TMA has 90 cores from 45 patients with invasive breast cancer, including 45 tumor tissues and 45 corresponding adjacent tissues. The immunohistochemical staining rate was classified as 0 (negative), 1 (1%-25% positive tumor cells), 2 (26%-50%), 3 (51%-75%), and 4 (76%-100%). Staining intensity was classified as 0 (absence of stained cells), 1 (weak staining), 2 (moderate staining), and 3 (strong staining). The immunohistochemistry (IHC) score was calculated by multiplying the staining rate and intensity. Correlations were determined by Spearman's coefficient of correlation.

3. Cell culture

MCF-7, adriamycin-resistant MCF-7 (MCF-7ADR), and MDA-MB-231 cell lines were purchased from the Cell Bank of the Chinese Academy of Sciences (Shanghai, China). Cell lines were validated using short tandem repeat analysis by Genesky Biotechnology Inc., Shanghai (Shanghai, China),

and tested for the absence of mycoplasma contamination by PCR using the Mycoplasma PCR Detection Kit. MCF-7 cells were maintained in MEM supplemented with 10% FBS, 0.01 mg/mL human recombinant insulin, and 1 μM nonessential amino acids. MCF-7ADR cells were cultured in RPMI-1640 medium supplemented with 10% FBS. MDA-MB-231 cells were cultured in L-15 medium supplemented with 15% FBS. Adriamycin was added on time to maintain the drug resistance phenotype of MCF-7ADR cells.

4. MTT assay

The MTT assay was used to measure the inhibitory effect of compounds on the viability of cancer cells. Adherent cells were seeded in 96-well plates at a density of 5,000 cells per well. After 24 hours, the cells were treated with different concentrations of triptolide for 72 hours. Twenty microliters of MTT solution was added to each well and incubated for 4 hours at 37°C. Then, dimethyl sulfoxide was added to the wells and incubated overnight at 37°C. The absorbance at 570 nm was measured using a microplate reader (BioTek, Winooski, VT).

5. Clinical dataset analysis

To analyze the expression of B4GalTs in invasive breast carcinomas compared with normal breast tissues, we used The Cancer Genome Atlas (TCGA) breast dataset from the Oncomine browser (https://www.oncomine.org).

Kaplan-Meier plotter (http://kmplot.com/analysis/index.php?p=background) was used to analyze the correlation between B4GalT5 expression and recurrence-free survival (RFS) in patients with breast cancer in 120 months [8].

The coexpression of B4GalT5 and CCR7, C-X-C chemokine receptor 4 (CXCR4), and ATP binding cassette subfamily B member 1 (ABCB1) was assessed in invasive breast invasive carcinoma samples from TCGA dataset by 'R2: Genomics Analysis and Visualization Platform' (http://r2.amc.nl). We also analyzed the coexpression of B4GalTs and ALDH1A1 and c-myc from GEPIA 2 from Zhang's lab [9]. Correlations were determined by Pearson's coefficient of correlation.

6. Flow cytometry analysis and sorting

For analysis of BCSC and non-BCSC cell fractions, cells were incubated with FITC-conjugated anti-CD44 antibody and PE or APC-conjugated anti-CD24 antibody in phosphate buffered saline (PBS) containing 2% FBS at 4°C for 30 minutes. BCSCs ($CD44^+CD24^{-/low}$) and non-BCSCs ($CD44^+CD24^+$) were analyzed and sorted by flow cytometry (MFLO XDP, Beckman Coulter, Pasadena, CA). The ALDEFLUOR Kit was used for the identification of BCSCs that express high levels of the enzyme aldehyde dehydrogenase (ALDH) according to the manufacturer's protocol.

For analysis of the proportions of the $CD24^{-/low}$ cell population in the His^+ cell population and His^- cell population, cells were incubated with PE-conjugated anti-His antibody and APC-conjugated anti-CD24 antibody in PBS containing 2% FBS at 4°C for 30 minutes. The samples were analyzed by flow cytometry (MFLO XDP, Beckman Coulter). The calculation method is as follows.

The proportion of $CD24^{-/low}$ cells in the His^+ cell population=$His^+CD24^{-/low}$ cells %/His^+ cells %.

The proportion of $CD24^{-/low}$ cells in the His^- cell population=$His^-CD24^{-/low}$ cells %/His^- cells %.

7. Plasmids

The DNA fragment for B4GalT5 was cloned from human cDNA using the corresponding primers and inserted into the pLVX-IRES-ZsGreen1 vector. The DNA fragment for B4GalT5-His was cloned from human cDNA using primers including His sequence and inserted into the pBABE-puro vector. These constructed vectors were transformed into DH5α cells and then amplified. The primers for B4GalT5 were 5′-CCGCTCGAGTGGCTGCAGCATGCGCG-3′ and 5′-CGCGGATCCTCAGTACTCGTTCACCTGAG-3′. The primers for B4GalT5-His were 5′-CGCGGATCCATGCGCGCCCGCCGGGGGCTGCT-3′ and 5′-CCGGAATTCTCAATGGTGATGGTGATGATGGT-3′.

8. siRNA and plasmid transfections

For siRNA transfection, cells were transfected at 80% confluency in 6-well plates with 50 nM control siRNA or B4GalT5-targeting siRNA (si-B4GalT5) (sense, 5′-CGGAGUGAGUGGCUUAACAdTdT-3′; antisense, 5′-UGUUAAGCCACUCACUCCGdTdT-3′) using Lipo2000 transfection reagents according to the manufacturer's instructions. The knockdown efficiency was examined by western blotting after 48 hours.

For plasmid transfection, cells were transfected with the plasmids using Lipo3000 transfection reagents according to the manufacturer's instructions. After 48 hours, the cells were treated with G418 or puromycin to screen for stably transfected MCF-7ADR cell lines. The stably transfected MCF-7ADR cell lines are as follows: B4GalT5-knockdown MCF-7ADR (MCF-7ADR/shB4GalT5), B4GalT5-overexpressing MCF-7ADR (MCF-7ADR/oe-B4GalT5), and MCF-7ADR expressing B4GalT5-His (MCF-7ADR/B4GalT5-His).

9. Mammosphere formation assay

For analysis of the effect of B4GalT5 on mammosphere formation, a single-cell suspension was quantified and seeded in ultralow attachment 6-well plates at a density of 2,000 cells per well at 37°C and 5% CO_2. Mammospheres were formed in serum-free DMEM/F-12 medium containing 20 ng/mL EGF, 10 ng/mL bFGF, 2% B27, and 5 μg/mL insulin. After 7 days, mammospheres with a diameter of > 50 μm were counted using a cell imaging multi-mode reader (BioTek).

For determination of the effect of triptolide on mammos-

pheres, single-cell suspensions were quantified and seeded in ultralow attachment 6-well plates at a density of 2,000 cells per well at 37°C and 5% CO_2. Mammospheres were formed in serum-free DMEM/F-12 medium containing 20 ng/mL EGF, 10 ng/mL bFGF, 2% B27, and 5 μg/mL insulin with treatment with PBS or different concentrations of triptolide. After 7 days, mammospheres with a diameter of > 50 μm were counted using a cell imaging multi-mode reader (Bio-Tek).

10. Colony formation assay

Five hundred microliters of pre-warmed 2×1,640 medium containing 20% FBS, 200 U/mL penicillin, 200 μg/mL streptomycin, and 500 μL of melted 1.2% agarose solution was mixed and transferred to a 6-well plate. When the bottom agar layer solidified, 1 mL of melted 0.7% agarose solution and 1 mL of single-cell suspension at a density of 500 cells per mL treated with increasing concentrations of triptolide were mixed and seeded on the bottom agar layer. The cells were incubated for 30 days at 37°C and 5% CO_2. The colonies were treated with 0.5 mL of MTT per well for 30 minutes at 37°C, and colonies containing up to 50 cells were counted.

11. Protein extraction, pull down, and immunoblotting

For the RCA-I pull-down assay, cells were lysed on ice for 30 minutes in cell lysis buffer for western and IP with 1 mM PMSF. Three hundred micrograms of total cell lysates were centrifuged at 12,000 ×g and 4°C for 10 minutes and then incubated with RCA-I agarose beads at 4°C overnight. After the samples were washed three times using cell lysis buffer, pulled-down proteins were subjected to western blotting. Total Frizzled-1 expression level was used as loading control.

For western blotting, membrane and cytosol proteins of MCF-7ADR cells were extracted by the membrane and cytosol extraction kit according to the manufacturer's instructions. Total cell lysates were prepared using loading buffer on ice for 45 minutes and denatured at 95°C for 15 minutes followed by sodium dodecyl sulfate polyacrylamide gel electrophoresis (SDS-PAGE). Then, the samples were transferred to Immobilon-P polyvinylidene difluoride membranes, blocked with 5% non-fat milk, and incubated with the indicated antibodies. SuperSignal West Femto Maximum Sensitivity Substrate was used to detect HRP-conjugated secondary antibodies.

12. Cell surface biotinylation assay

After the samples were washed twice with cold PBS, MCF-7ADR cells were incubated with EZ-Link Sulfo-NHS-SS-Biotin at a final concentration of 0.5 mg/mL for 60 minutes at 4°C, followed by a 50 mM glycine/PBS wash and two washes with PBS. Biotinylated cells were lysed with cell lysis buffer for western and IP and then centrifuged for 15 minutes at 12,000 ×g and 4°C. The supernatant was incubated with PNeutrAvidin agarose beads and mixed at 4°C overnight. Biotinylated proteins were eluted from the beads by heating to 100°C for 5 minutes in SDS-PAGE sample buffer before loading into the SDS-PAGE gel for western blotting.

13. Immunofluorescence assay

For detection of the p-GSK3β (Ser 9) and B4GalT5 expression levels, cells were cultured on a 96-well black-wall glass bottom plate for 24 hours. They were fixed with 4% paraformaldehyde for 30 minutes, permeabilized with 0.3% Triton X-100 for 20 minutes and blocked with 1% bovine serum albumin (BSA) in PBS for 1 hour. The cells were incubated with primary antibody (1:50) in blocking buffer. After sufficient washing, the cells were incubated with FITC-conjugated goat anti-rabbit antibody to detect the primary antibody. The cells were incubated with DAPI for 10 minutes. The resulting images were taken using a laser scanning confocal microscope (Carl Zeiss, Jena, Germany).

For detection of B4GalT5-His and CD24 on the cell surface, the cells were digested and resuspended in 1% BSA in PBS. The cells were incubated with anti-His antibody (1:50) in 1% BSA. After sufficient washing, the cells were incubated with FITC-conjugated goat anti-rabbit antibody and APC-conjugated anti-CD24 antibody for 1 hour. The resulting images were taken using a laser scanning confocal microscope (Carl Zeiss).

14. Animal studies

MCF-7ADR/NC and B4GalT5-overexpressing MCF-7ADR (MCF-7ADR/oe-B4GalT5) cells were subcutaneously transplanted into 14-15 g, 6-week-old female BALB/c nude mice (Beijing Vital River Laboratory Animal Technology Co., Ltd., Beijing, China) at a concentration of 2×10^6 cells per site. Five mice were used in each group for analysis of B4GalT5-induced tumor initiation. The tumor volumes of these mice were measured every week to assess tumor initiation and growth. These tumors were dissected 9 weeks after transplantation and weighed. Then, these tumors were excised, ground, and lysed in loading buffer on ice for 45 minutes. Protein lysates were boiled for 10 minutes and then subjected to western blotting.

15. Statistical analysis

Statistical comparisons between two groups were performed by two-tailed Student's t tests. The means were calculated using at least three biological replicates. Error bars represent the standard error of the mean for three independent experiments. p-values of < 0.05 were considered statistically significant.

16. Ethical statement

This study was approved by School of Medicine and Pharmacy, Ocean University of China, and performed in accord-

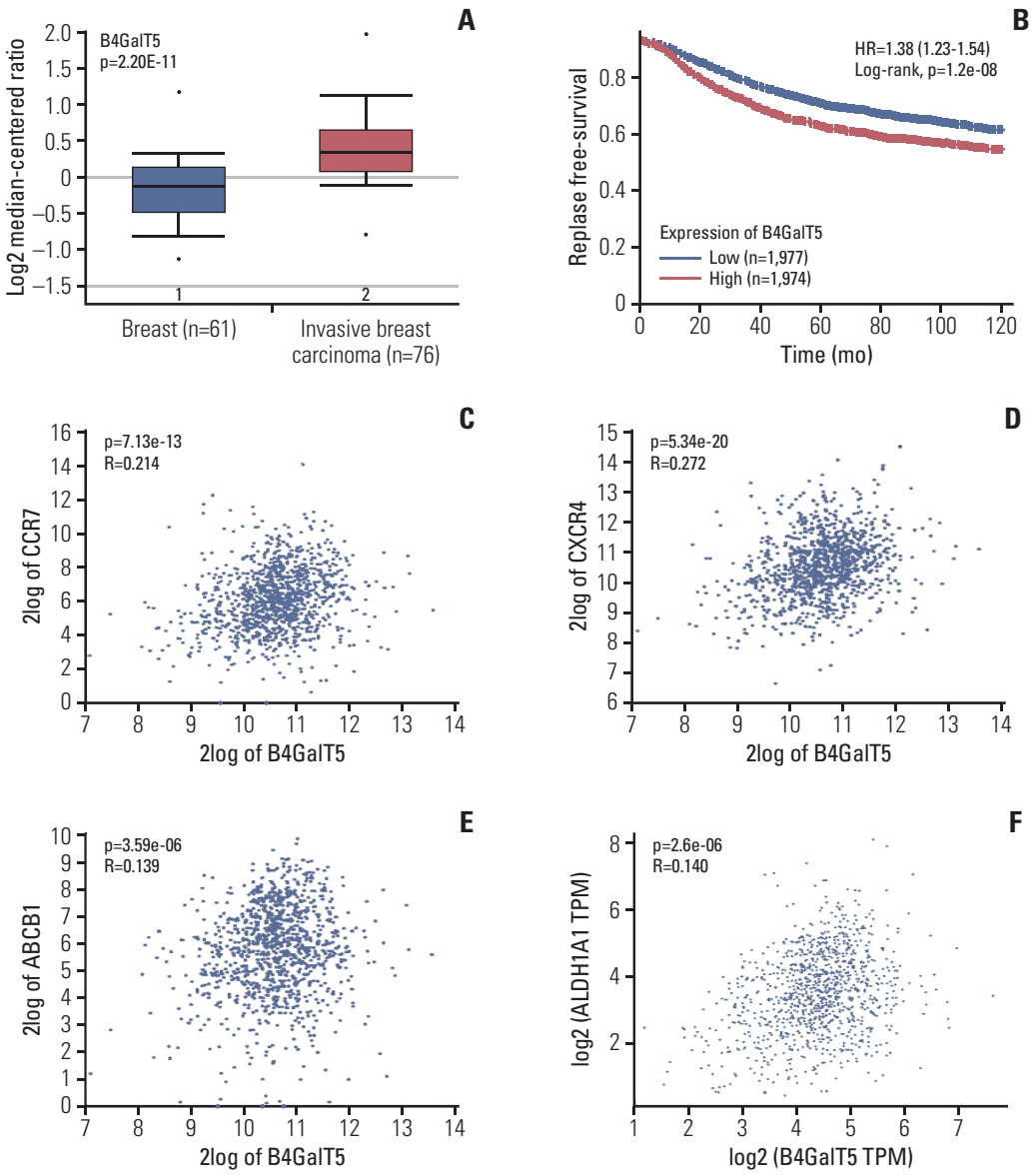

Fig. 1. β1,4-Galactosyltransferase V (B4GalT5) is associated with the stemness of breast cancer. (A) The Cancer Genome Atlas (TCGA) breast dataset analysis of B4GalT5 mRNA levels in invasive breast carcinomas (n=76) and normal breast tissues (n=61) using the Oncomine browser. (B) Kaplan-Meier survival curves for patients with breast cancer (n=3,955) in 120 months. The correlation between B4GalT5 expression and relapse-free survival of patients with breast cancer were analyzed using Kaplan-Meier plotter. (C-E) Correlation between B4GalT5 and CC-chemokine receptor 7 (CCR7) (C), C-X-C chemokine receptor 4 (CXCR4) (D), or ATP binding cassette subfamily B member 1 (ABCB1) (E) mRNA levels in invasive breast carcinoma samples from TCGA dataset (n=1,097) using 'R2: Genomics Analysis and Visualization Platform.' (F) The correlation between B4GalT5 and aldehyde dehydrogenase 1A1 (ALDH1A1) mRNA levels in breast carcinoma patients from TCGA dataset using GEPIA 2. *(Continued to the next page)*

ance with the National Institutes of Health Guide for the Care and Use of Laboratory Animals (NIH publication, 8th edition, 2011).

Results

1. B4GalT5 is associated with the stemness of breast carcinoma

To investigate the relationship between B4GalT5 and BCSCs, we first used online database analysis to compare the B4GalT5 expression level in invasive breast carcinomas with that in normal breast tissues, as CSCs are thought to be close-

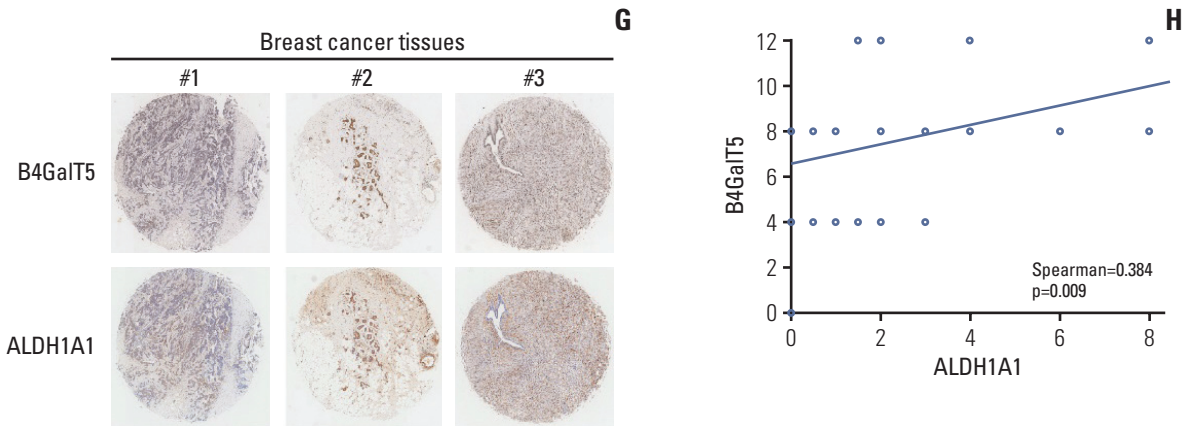

Fig. 1. *(Continued from the previous page)* (G) Representative images of B4GalT5 and ALDH1A1 expression in the breast tumor microarray by immunohistochemistry (IHC) analysis. (H) The correlation between B4GalT5 and ALDH1A1 IHC scores of 45 cores of the breast tumor microarray.

Table 1. B4GalTs mRNA levels in invasive breast carcinomas (n=76) and normal breast tissues (n=61)

Gene	Fold change (vs. normal)	p-value[a)]
B4GalT1	1.579	9.65e-7
B4GalT2	1.589	1.91e-9
B4GalT3	2.059	7.05e-27
B4GalT4	1.393	2.50e-9
B4GalT5	1.507	2.20E-11
B4GalT6	–1.615	1.000
B4GalT7	1.459	1.48e-6

B4GalT, β1,4-galactosyltransferase V. [a)]$p < 0.01$, statistically significant.

Table 2. Correlation between B4GalTs and ALDH1A1 in breast carcinoma samples from TCGA breast dataset

Gene	r (Pearson)[a)]	p-value[b)]
B4GalT1	–0.026	0.39
B4GalT2	–0.091	0.0026
B4GalT3	–0.038	0.21
B4GalT4	0.034	0.27
B4GalT5	0.14	2.6e-06
B4GalT6	0.2	2.4e-11
B4GalT7	–0.042	0.16

B4GalT, β1,4-galactosyltransferase V; ALDH1A1, aldehyde dehydrogenase 1A1; TCGA, The Cancer Genome Atlas. [a)]$r > 0$, positive correlation; $r < 0$, negative correlation, [b)]$p < 0.01$, statistically significant.

ly correlated with the migration and invasiveness of cancer cells [2]. The TCGA breast dataset showed that B4GalT5 was highly expressed in invasive breast carcinomas (Fig. 1A). Kaplan-Meier survival curves for patients with breast cancer (n=3,955) also showed that patients with high expression of B4GalT5 had lower RFS than those with low expression (Fig. 1B, S1 Table). Because BCSCs can establish metastasis and evade traditional anti-tumor therapies [2], we further examined the correlation between B4GalT5 and these malignant phenotypes. Online database analysis showed a positive correlation between B4GalT5 and CC-chemokine receptor 7 (CCR7; R=0.214, p=7.13e-13) (Fig. 1C), CXCR4 (R=0.272, p=5.34e-20) (Fig. 1D), and multidrug resistance protein 1 (ABCB1) (R=0.139, p=3.59e-06) (Fig. 1E), which are involved in tumor metastasis and chemoresistance [10,11]. These results indicate that B4GalT5 is correlated with cancer progression and may be related to BCSCs. ALDH1A1 is related to cancer stem-like features and its high expression and activity has also been proposed as a reliable CSC marker [12]; therefore, we further detected the correlation between B4GalT5 and ALDH1A1. We found that B4GalT5 was positively associated with ALDH1A1 (R=0.14, p=2.6e-06) (Fig. 1F). Since the B4GalT family has seven members, we further investigated the relationship of other B4GalTs and the malignancy of breast carcinoma by online database analysis and found that most B4GalTs (except B4GalT6) were highly expressed in invasive breast carcinomas compared with normal breast tissues (Table 1). Of note, B4GalT5 was the only member positively correlated with the BCSC marker ALDH1A1 (Table 2). For further verification, the expression of B4GalT5 and ALDH1A1 was detected in a tumor microarray containing 45 cancer tissues from patients with invasive breast cancer. Pathologic information regarding these patients is presented in S2 Table. There was a positive correlation between B4GalT5 and ALDH1A1 expression (Spearman=0.384, p=0.009) in 45 patients (Fig. 1G and H). Collectively, these results suggest a critical role of B4GalT5 in regulating the stemness of BCSCs.

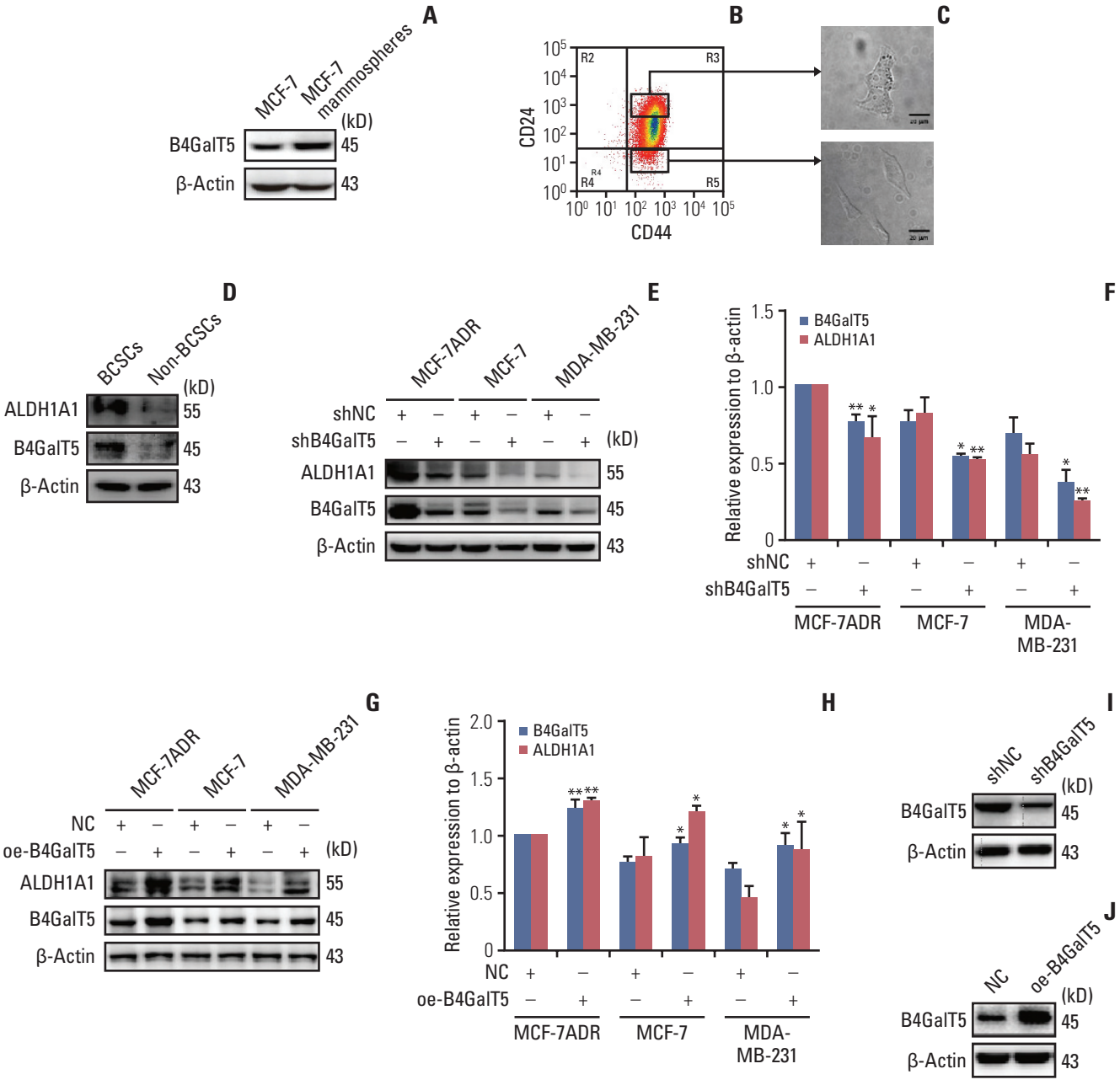

Fig. 2. β1,4-Galactosyltransferase V (B4GalT5) is required for maintaining the stemness of breast cancer. (A) Western blotting analysis of B4GalT5 expression levels in intact MCF-7 cells and MCF-7 mammospheres. (B) Flow cytometry (FCM) analysis and sorting of $CD44^{+}CD24^{-/low}$ cells (breast cancer stem cells [BCSCs]) and $CD44^{+}CD24^{+}$ cells (non-BCSCs) in MCF-7ADR cells. (C) Patterns of BCSCs and non-BCSCs sorted from MCF-7ADR cells. Scale bars=20 μm. (D) Western blotting analysis of B4GalT5 and aldehyde dehydrogenase 1A1 (ALDH1A1) expression levels in BCSCs and non-BCSCs sorted from MCF-7ADR cells. (E-H) Effects of B4GalT5 on ALDH1A1 expression in breast cancer cells by western blotting. MCF-7, MCF-7ADR, and MDA-MB-231 cells were transfected using shB4GalT5 (E, F) or B4GalT5 (G, H) plasmids for 48 hours and subjected to western blotting compared to the negative control. Protein band densities were quantified by normalizing to β-actin. (I, J) Expression levels of B4GalT5 in MCF-7ADR/shB4GalT5 (I) and MCF-7ADR/oe-B4GalT5 (J) compared to the negative control. *(Continued to the next page)*

2. B4GalT5 is required for maintaining the stemness of breast cancer

To further investigate the relationship between B4GalT5 and BCSCs, we performed *in vitro* studies using MCF-7 and MCF-7ADR breast cancer cell lines. CSCs can form mammospheres in serum-free culture medium supplemented

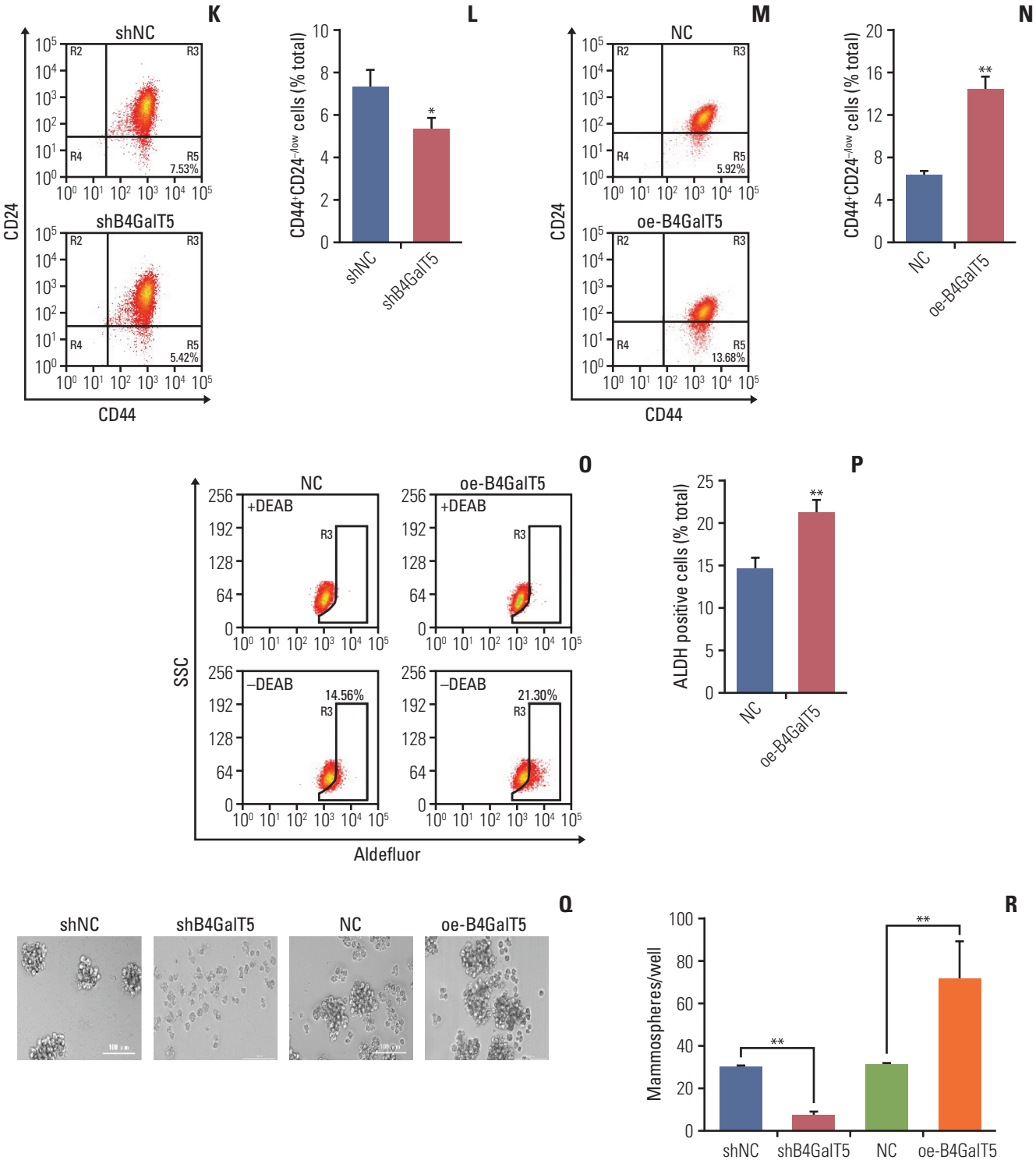

Fig. 2. *(Continued from the previous page)* (K-N) Influences of B4GalT5 on the proportion of $CD44^{+}CD24^{-/low}$ cells in MCF-7ADR/shB4GalT5 (K, L) or MCF-7ADR/oe-B4GalT5 (M, N) cells compared to the negative control. Cells were stained with anti-CD44 and anti-CD24 antibodies and analyzed by FCM. (O, P) FCM analysis of ALDH+ cells in MCF-7ADR/oe-B4GalT5 cells compared to MCF-7ADR/NC cells. The cells were stained and analyzed as described. (Q, R) The sizes and numbers of mammospheres formed by MCF-7ADR/shB4GalT5 and MCF-7ADR/oe-B4GalT5 compared to the negative control groups. Two thousand cells per well were cultured in serum-free medium for seven days. Formed mammospheres were quantified, and images of formed spheres with a diameter of > 50 μm were taken with a light microscope. Scale bars=100 μm. *(Continued to the next page)*

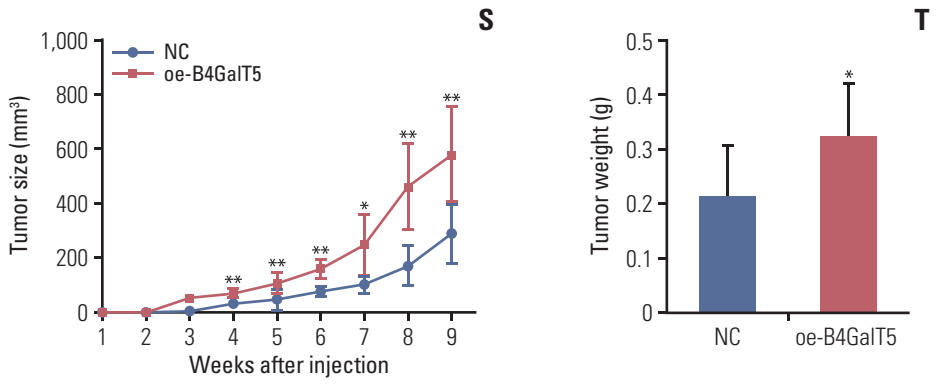

U

Days after injection	1	28	35	42	49	56	63
NC	0/5	0/5	0/5	0/5	2/5	3/5	5/5
oe-B4GalT5	0/5	3/5	4/5	5/5	5/5	5/5	5/5

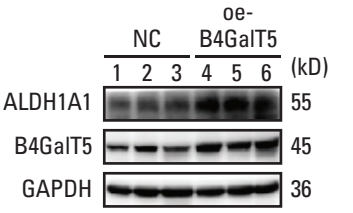

Fig. 2. *(Continued from the previous page)* (S, T) Volumes (S) and weights (T) of tumor formed by MCF-7ADR/NC and MCF-7ADR/oe-B4GalT5 cells in BALB/c nude mice. MCF-7ADR/NC and MCF-7ADR/oe-B4GalT5 cells were subcutaneously transplanted into female BALB/c nude mice at the concentration of 2×10^6 cells per site. After 9 weeks, the mice were sacrificed for measurement of tumor weights (n=5, per group). (U) Statistics of tumors with a volume of 100 mm^3 after subcutaneous injection of MCF-7ADR cells. (V) Western blotting analysis of B4GalT5 and ALDH1A1 expression in tumor tissues. All experiments were performed in three replicates. All data are representative and shown as means±standard error of the mean. *$p < 0.05$, **$p < 0.01$, vs. negative control (NC).

with appropriate growth factors due to their capacity for self-renewal and multipotent differentiation; the mammosphere formation assay is also widely used in the isolation and enrichment of CSCs. First, we compared the B4GalT5 expression in MCF-7 mammospheres versus intact MCF-7 cells. As shown in Fig. 2A, western blotting analysis showed that B4GalT5 was highly expressed in the MCF-7 mammospheres.

Because $CD44^+CD24^{-/low}$ is identified as the molecular marker of BCSCs [2], we next verified whether the expression of B4GalT5 was associated with $CD44^+CD24^{-/low}$ cells. Multiple forms of drug resistance induced by continuous exposure of cells to chemotherapeutics usually generate a high proportion of BCSCs [13]. We therefore chose the adriamycin-resistant breast cancer cell line MCF-7ADR for further research. $CD44^+CD24^{-/low}$ cells (BCSCs) and $CD44^+CD24^+$ cells (non-BCSCs) were sorted from MCF-7ADR cells aseptically by flow cytometry (Fig. 2B), cultured and subjected to western blotting. Strikingly, the $CD44^+CD24^{-/low}$ cells displayed a more malignant phenotype than the $CD44^+CD24^+$cells and had a spindle shape and limited cell-cell contacts; in contrast, the $CD44^+CD24^+$ cells displayed a cobblestone epithelial morphology (Fig. 2C), which is consistent with a previous report showing that $CD44^+CD24^{-/low}$ cells were representative of BCSCs. Furthermore, western blotting analysis showed that B4GalT5 was significantly overexpressed in the $CD44^+CD24^{-/low}$ cells versus the $CD44^+CD24^+$ cells; in addition, the BCSC marker ALDH1A1 was increased along with overexpression of B4GalT5 (Fig. 2D). Together, these results indicate that B4GalT5 is highly expressed in BCSCs.

To explore the role of B4GalT5 in regulating the stemness of BCSCs, we first detected the effect of B4GalT5 on stem cell marker ALDH1A1 expression in breast cancer cells and found an obvious reduction in ALDH1A1 expression in MCF-7ADR, MCF-7, and MDA-MB-231 cell lines (Fig. 2E and F). In contrast, B4GalT5 overexpression (oe-B4GalT5) significantly augmented ALDH1A1 expression in breast cancer cells (Fig. 2G and H). Moreover, we constructed MCF-7ADR cells with stable knockdown of B4GalT5 (referred to as shB4GalT5, Fig. 2I) and stable overexpression of B4GalT5 (referred to as oe-B4GalT5) (Fig. 2J), followed by *in vitro* and *in vivo* studies. We observed a significant decline in the $CD44^+CD24^{-/low}$ cells (Fig. 2K and L) in shB4GalT5 cells, as previously observed in siB4GalT5 transfected MCF-7ADR cells. In contrast, B4GalT5 overexpression significantly increased the percentage of $CD44^+CD24^{-/low}$ cells (Fig. 2M and N), accompanied by increased ALDH activity (Fig. 2O and P), indicating that B4GalT5 induces the formation of BCSC stemness. Moreover, we performed a mammosphere formation assay to assess the self-renewal ability of BCSCs and the expression

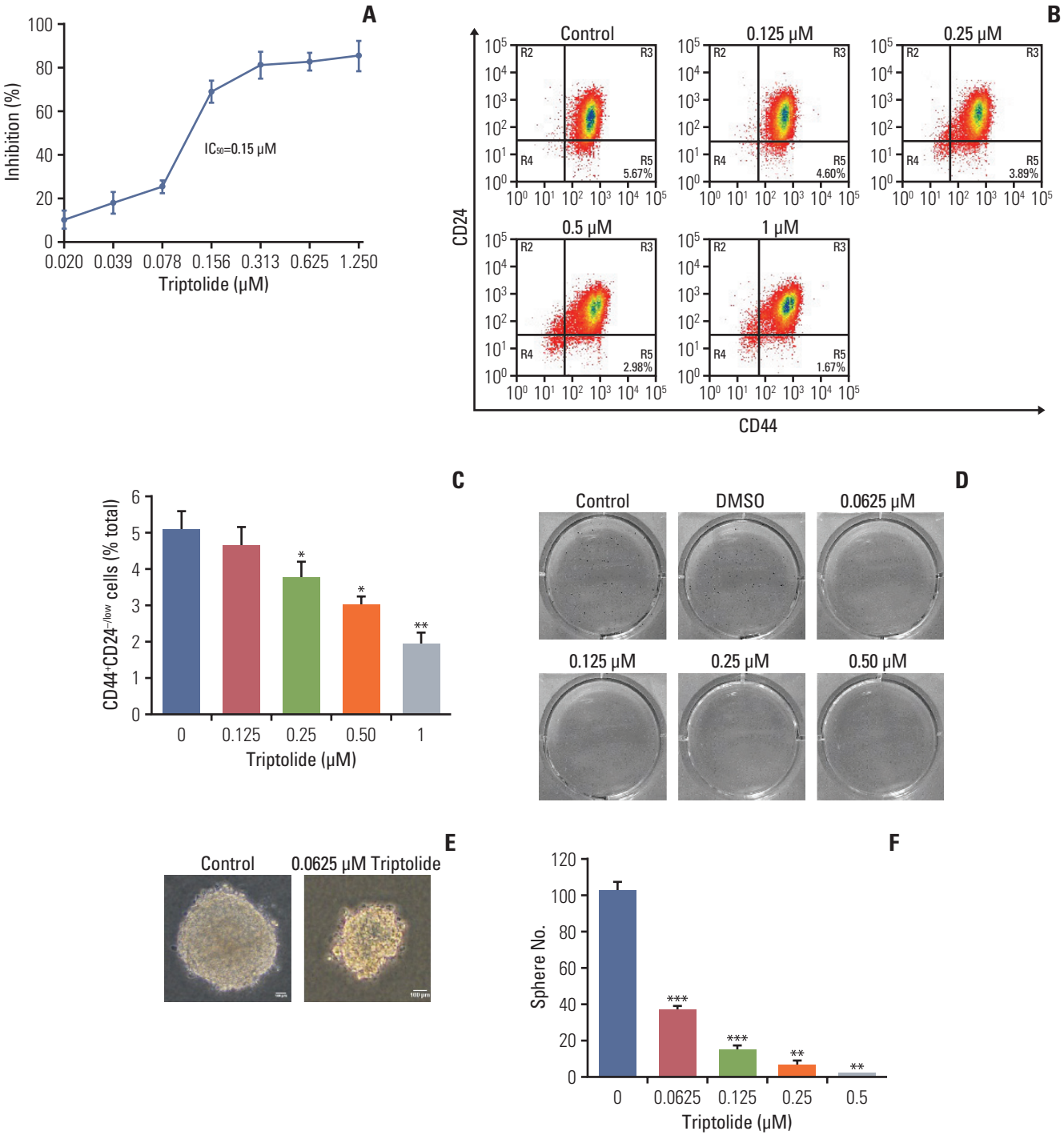

Fig. 3. β1,4-Galactosyltransferase V (B4GalT5) is involved in the inhibition of breast cancer stem cells by triptolide. (A) IC_{50} of triptolide against MCF-7ADR cells using MTT assay. Cells were treated with increasing concentrations of triptolide for 72 hours and MTT assay was performed. NC, normal control. (B, C) Inhibitory effect of triptolide on the proportion of $CD44^{+}CD24^{-/low}$ cells in MCF-7ADR cells. Cells were treated with increasing concentrations of triptolide for 48 hours, then stained with anti-CD44 and anti-CD24 antibodies and analyzed by flow cytometry. (D) Images of colonies in the soft agar. Five hundred MCF-7ADR cells per well were plated in the upper agar for 30 days with the treatment with triptolide before MTT dye was added. Images of formed colonies containing up to 50 cells with a light microscope are shown. (E) Images of colonies magnified treated with dimethyl sulfoxide (DMSO) or 0.0625 μM triptolide using a light microscope. Scale bars=100 μm. (F) Quantification of the number of colonies. *(Continued to the next page)*

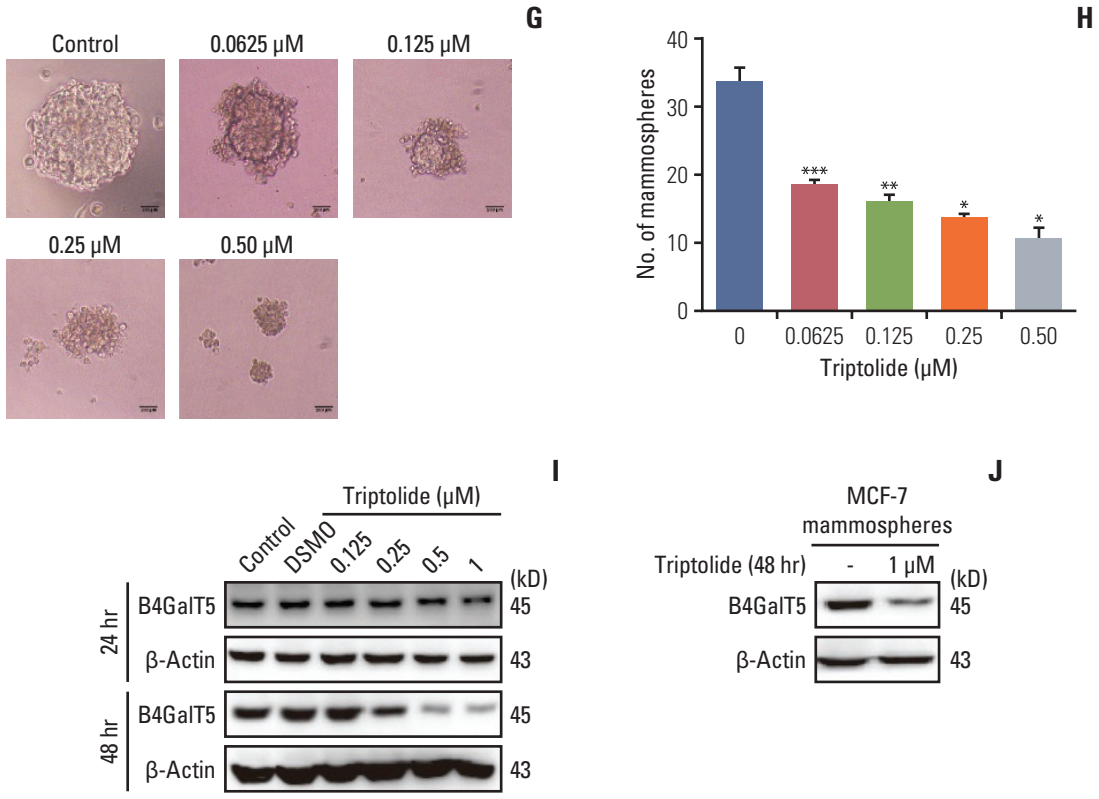

Fig. 3. *(Continued from the previous page)* (G) Images of mammospheres in serum-free medium. 2000 MCF-7 cells per well were cultured in serum-free medium with treatment with phosphate buffered saline (PBS) or different concentrations of triptolide. After 7 days, pictures were taken using light microscopy with a camera. Scale bars=200 μm. (H) Quantification of the number of colonies. (I) Inhibitory effect of triptolide on B4GalT5 expression in MCF-7ADR cells in dose- and time-dependent manners. MCF-7ADR cells were treated with different concentrations of triptolide for 24 hours and 48 hours. Then cells were subjected to western blotting. (J) Inhibitory effect of triptolide on B4GalT5 expression in MCF-7 mammospheres by western blotting. All experiments were performed in three replicates. All data are representative and shown as means±standard error of the mean. *$p < 0.05$, **$p < 0.01$, ***$p < 0.001$, vs. the former group.

level of B4GalT5. We found that the size and number of the mammospheres were markedly restrained in the shB4GalT5 cells, whereas B4GalT5 overexpression promoted the formation of mammospheres (Fig. 2Q and R). It has been reported that CSCs drive tumor initiation, progression, and recurrence [2]. We then subcutaneously injected constructed MCF-7ADR cells into female BALB/c nude mice and found that the group with B4GalT5 overexpression exhibited a dramatic increase in tumor growth and weight compared with the control group (Fig. 2S and T). Specifically, the oe-B4GalT5 cells formed tumors with a volume of 100 mm^3 volume earlier than the cells without B4GalT5 overexpression, as plotted in Fig. 2U, further highlighting the strong tumorigenicity conferred by B4GalT5. Furthermore, we found that tumor tissue with B4GalT5 overexpression had higher expression levels of ALDH1A1, as assessed by western blot, than the tissues of the control group (Fig. 2V). Consequently, these results confirm that B4GalT5 plays an important role in maintaining the stemness of BCSCs.

3. B4GalT5 is involved in the inhibition of BCSCs by triptolide

Triptolide, a diterpene triepoxide of extracts derived from the medicinal plant *Tripterygium Wilfordii Hook F*, has been reported to inhibit the stemness of various cancers, including triple-negative breast cancer and pancreatic cancer [14]. Therefore, we wondered whether B4GalT5 was involved in the inhibition of BCSCs by triptolide. We found that MCF-7ADR cell viability was inhibited by treatment with triptolide, with an IC_{50} of 0.15 μM (Fig. 3A). In addition, triptolide dramatically reduced the percentage of $CD44^+CD24^{-/low}$ cells, suggesting that triptolide significantly eliminated BCSCs (Fig. 3B and C). Furthermore, we found that triptolide apparently suppressed colony growth in soft agar (Fig. 3D-F) and the formation of mammospheres in serum-free medium supplemented with certain cytokines (Fig. 3G and H). All these results confirmed that triptolide was indeed a pharmacological inhibitor of BCSCs. We further investigated whether inhibition of BCSCs by triptolide was accompanied by a decrease in B4GalT5. In the presence of triptolide, the

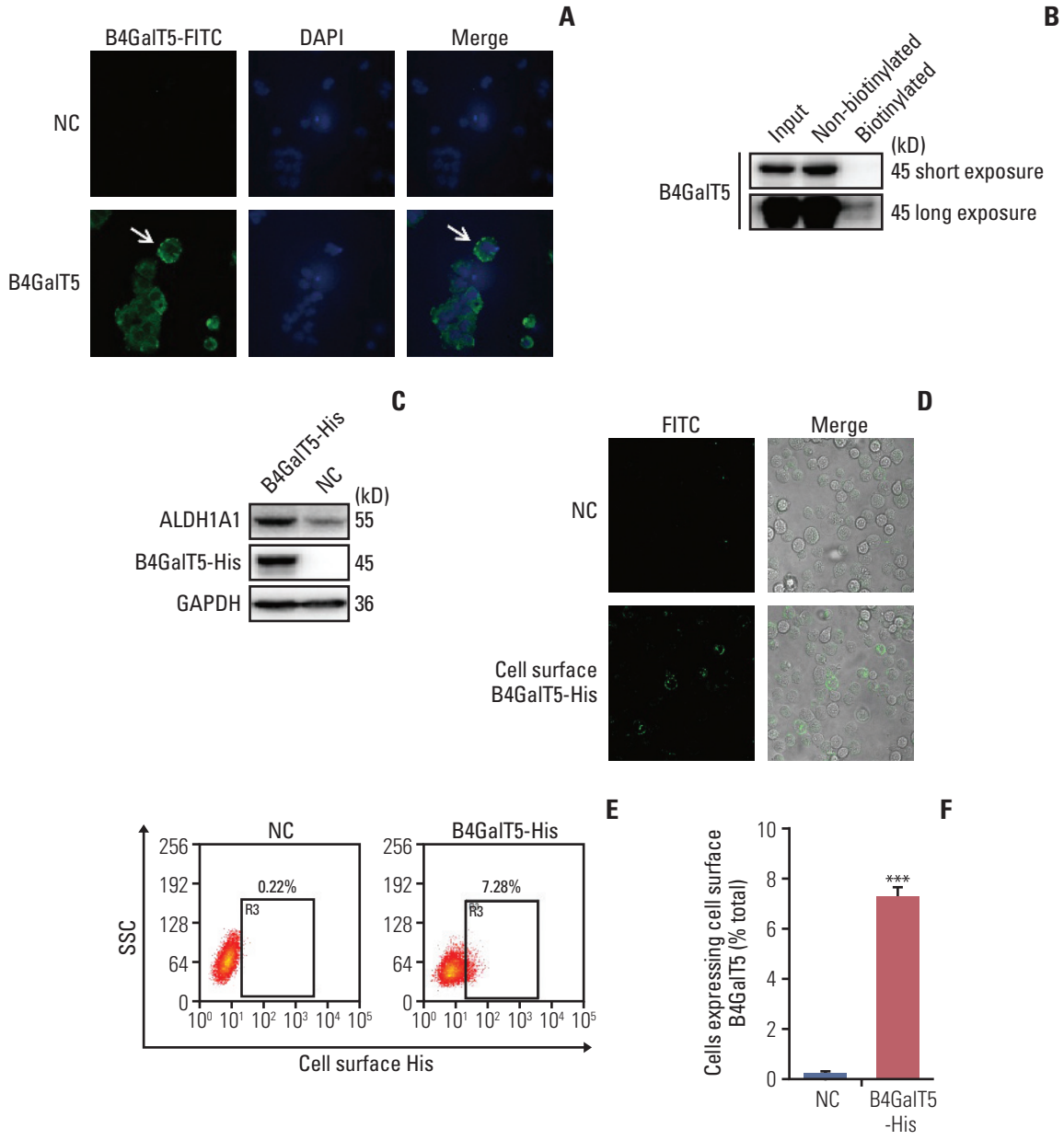

Fig. 4. Cell surface β1,4-galactosyltransferase V (B4GalT5) is not responsible for the stemness of breast cancer. (A) Immunofluorescence analysis of B4GalT5 expression in MCF-7ADR cells. Cells were stained with IgG or anti-B4GalT5 antibody followed by fluorescein isothiocyanate (FITC)–conjugated anti-Rabbit antibodies as described and analyzed by a laser scanning confocal microscope. (B) Cell surface biotinylation assay to compare B4GalT5 localization in plasma membrane and cytoplasmic fractions of MCF-7ADR cells. (C) Construction of MCF-7ADR cells that stably expresses B4GalT5 with a C-terminal 6×His tag. MCF-7ADR cells were transfected with pBABE-B4GalT5-His-IRES-puro plasmid for 48 hours and then selected with 150 μg/mL puromycin. Expression of corresponding proteins was examined by western blotting. (D) Representative images of B4GalT5-His expression on the cell surface of MCF-7ADR/B4GalT5-His and MCF-7ADR/NC cells. After digested and resuspended, the cells were stained with anti-His antibody at room temperature for 1 hour followed by FITC-conjugated anti-rabbit antibody at room temperature for 1 hour. Pictures were taken by a laser scanning confocal microscope. (E, F) Flow cytometry (FCM) analysis of B4GalT5-His expression on the cell surface of MCF-7ADR/B4GalT5-His and MCF-7ADR/NC cells. Cells were stained with phycoerythrin (PE)-conjugated anti-His antibody at room temperature for 1 hour and analyzed by Moflo XDP. Error bars represent standard error of the mean (n=3, ***$p < 0.001$, t test). *(Continued to the next page)*

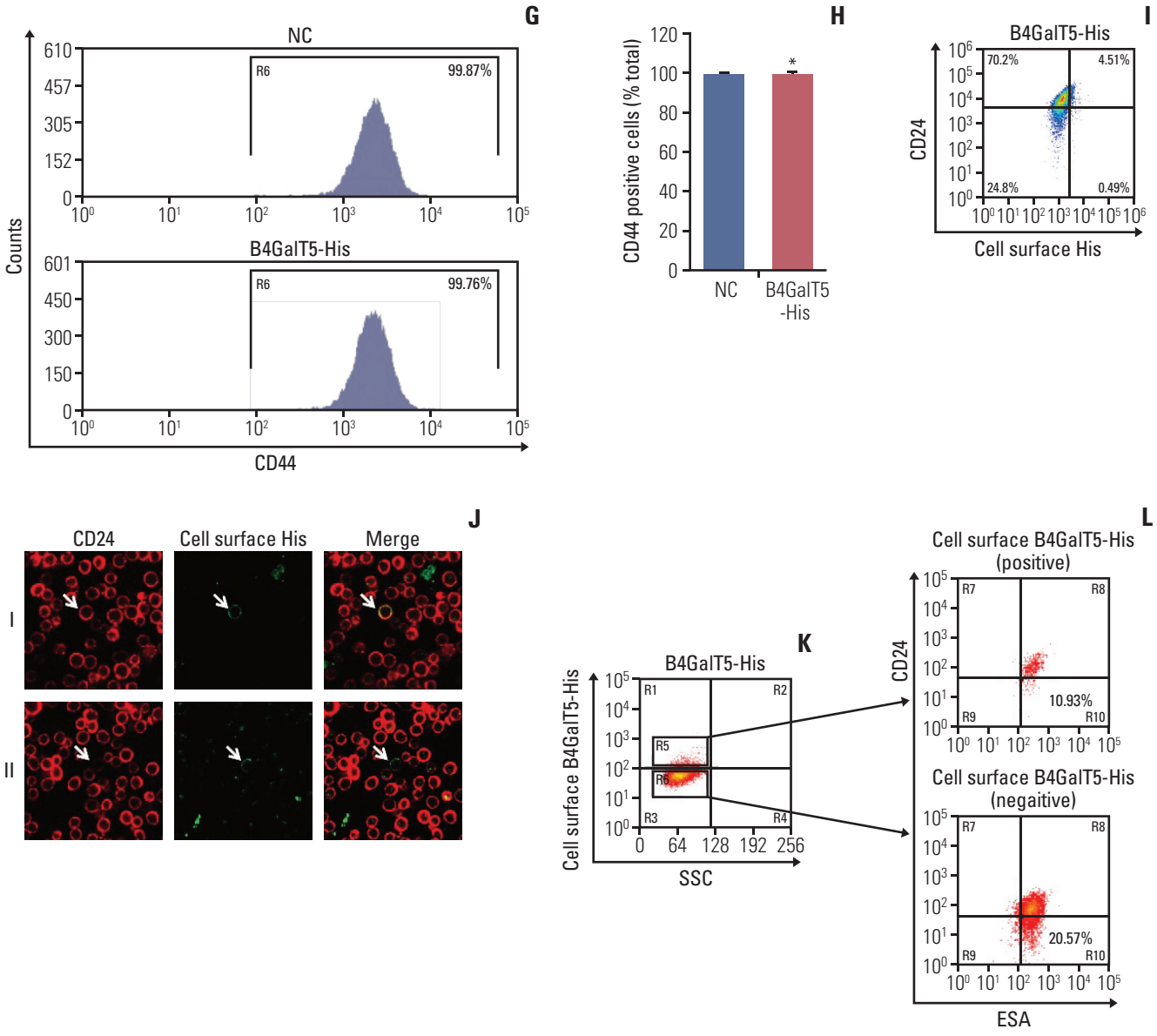

Fig. 4. *(Continued from the previous page)* (G, H) FCM analysis of CD44 expression in MCF-7ADR/B4GalT5-His and MCF-7ADR/NC cells. The cells were stained with FITC-conjugated CD44 antibody at 4°C for 30 minutes and analyzed using Moflo XDP. Error bars represent SEM (n=3; *p > 0.05, t test). (I) FCM analysis of $CD24^{-/low}$ cells in B4GalT5-His positive on the cell surface of MCF-7ADR/B4GalT5-His cells. MCF-7ADR/B4GalT5-His and MCF-7ADR/NC cells were stained with APC-conjugated anti-CD24 and PE-conjugated anti-His antibodies and analyzed by Moflo XDP. (J) Representative images of CD24 and B4GalT5-His expression on the cell surface of MCF-7ADR/B4GalT5-His and MCF-7ADR/NC cells. After digested and resuspended, the cells were stained with anti-CD24 and anti-His antibodies. Pictures were taken by a laser scanning confocal microscope. (K, L) FCM analysis of $ESA^{+}CD24^{-/low}$ cells in B4GalT5-His positive (K, R5) and negative (K, R6) on the cell surface of MCF-7ADR/B4GalT5-His cells; NC, negative control; GAPDH, glyceraldehyde 3-phosphate dehydrogenase; SSC, Side Scatter; ESA, epithelial specific antigen. All experiments were performed in three replicates.

expression level of B4GalT5 was significantly decreased in a dose- and time-dependent manner (Fig. 3I). In particular, B4GalT5 expression in MCF-7 mammospheres was inhibited by treatment with 1 μM triptolide (Fig. 3J). Together, these results further indicate that B4GalT5 is closely correlated with the stemness of breast cancer.

4. Cell surface B4GalT5 is not responsible for the stemness of breast cancer

It has been reported that B4GalT show cell surface expression for cell spreading and migration in migratory 3T3 cells [15], indicating that cell surface B4GalTs correlates with cancer malignancy. Thus, we tested whether cell sur-

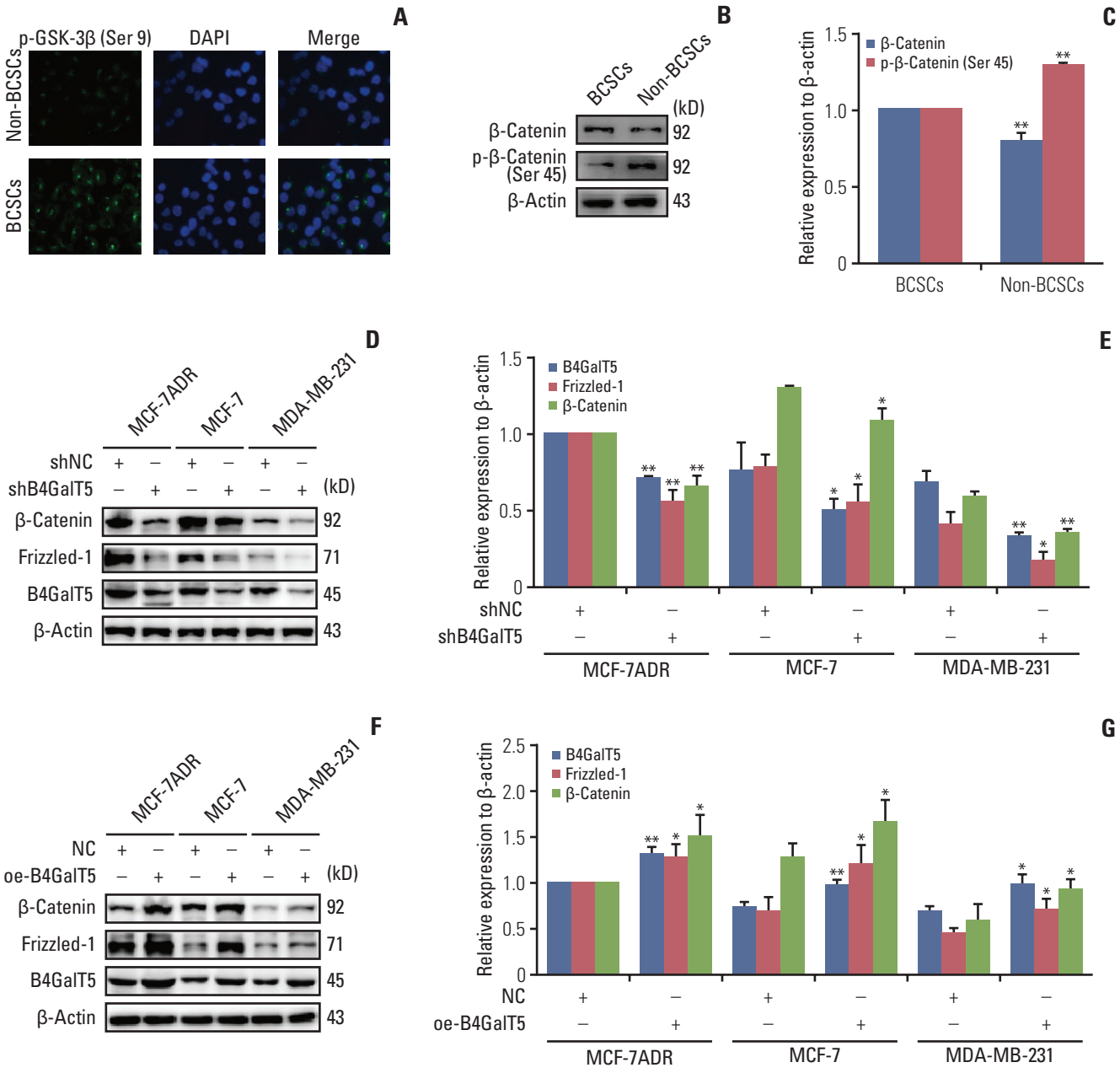

Fig. 5. β1,4-Galactosyltransferase V (B4GalT5) promotes Wnt/β-catenin signaling that is hyperactivated in breast cancer stem cells (BCSCs). (A) Immunofluorescence analysis of phosphorylated-GSK3β (Ser 9) expression in BCSCs and non-BCSCs. MCF-7ADR cells were sorted into BCSCs and non-BCSCs, then stained with antibodies and DAPI as described and analyzed by a laser scanning confocal microscope. (B, C) Western blotting analysis of β-catenin and phosphorylated-β-catenin (Ser 45) expression levels in BCSCs and non-BCSCs. Protein band densities were quantified by normalizing to β-actin. (D, E) The effect of B4GalT5 knockdown on Frizzled-1, β-catenin, and B4GalT5 expression levels in MCF-7ADR, MCF-7, and MDA-MB-231 cell lines by western blotting analysis. Protein band densities were quantified by normalizing to β-actin. (F, G) The effect of B4GalT5 overexpression on Frizzled-1, β-catenin, and B4GalT5 expression levels in MCF-7ADR, MCF-7, and MDA-MB-231 cell lines by western blotting analysis. Protein band densities were quantified by normalizing to β-Actin. *(Continued to the next page)*

face B4GalT5 was correlated with the stemness of BCSCs. As shown in Fig. 4A, cell surface B4GalT5 was found in a small portion of MCF-7ADR cells by confocal microscopy. Further, we carried out a cell surface biotinylation assay and proved that the expression level of cell surface B4GalT5 was much lower than that of cytoplasmic B4GalT5 in MCF-7ADR cells (Fig. 4B), indicating that a small proportion of the cells expresses cell surface B4GalT5. These results were consist-

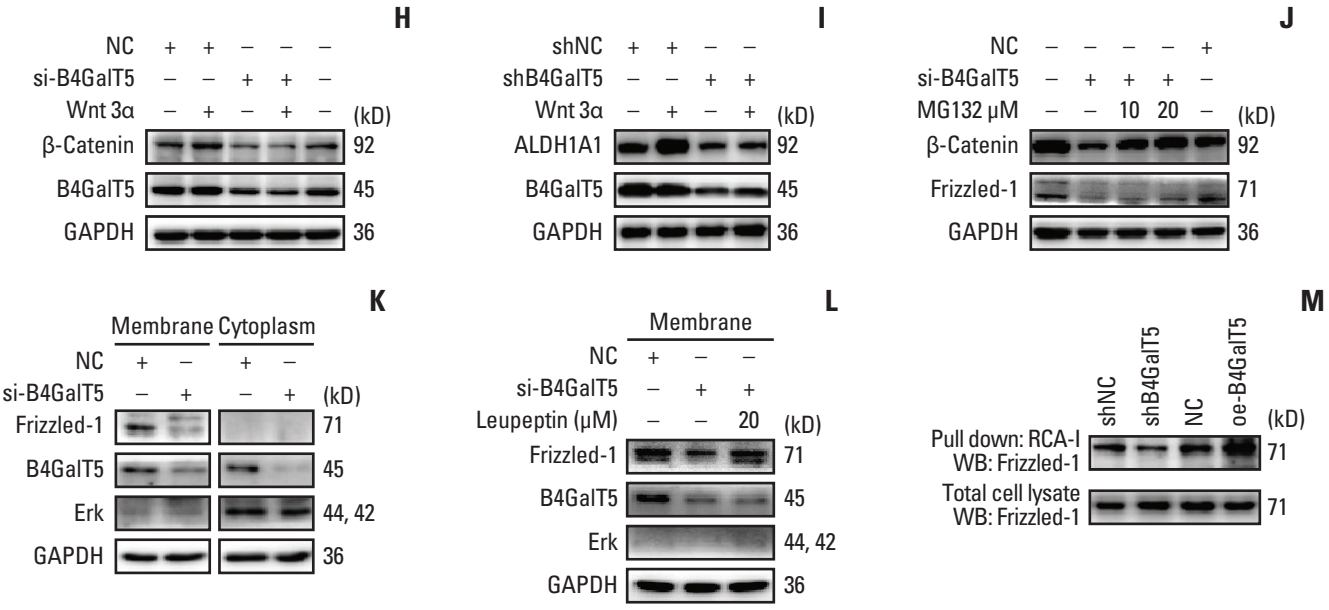

Fig. 5. *(Continued from the previous page)* (H) The effect of B4GalT5 on wnt 3α induced Wnt/β-catenin signaling by western blotting (WB). After transfected using B4GalT5 siRNA for 12 hours, MCF-7ADR cells were starved for 36 hours followed by adding wnt 3α, and subjected to western blotting. (I) The effect of B4GalT5 on Wnt 3α induced ALDH1A1 expression by western blotting. MCF-7ADR/shNC and MCF-7ADR/shB4GalT5 cells were starved for 36 hours followed by adding Wnt 3α, and subjected to western blotting. (J) The degradation pathway of β-catenin due to B4GalT5 knockdown. After transfected using B4GalT5 siRNA for 41 hours, MCF-7ADR cells were treated with MG132 (protease inhibitor) for 7 hours. Protein levels were examined by western blotting. (K) Western blotting analysis of membrane and cytosol proteins in MCF-7ADR cells. MCF-7ADR cells were transfected using B4GalT5 siRNA for 48 hours, extracted into membrane and cytosol proteins and then subjected to western blotting. Erk was used for examining purity of membrane proteins. (L) The degradation pathway of Frizzled-1 on the cell surface of MCF-7ADR cells due to B4GalT5 knockdown. After transfected using B4GalT5 siRNA for 40 hours, MCF-7ADR cells were treated with 20 μM leupeptin (lysosome inhibitor) for 8 hours. The membrane proteins were extracted as described and then subjected to western blotting. Erk was used for examining purity of membrane proteins. (M) The effect of B4GalT5 on biosynthesis of galactosyl-oligosaccharides in glycans of Frizzled-1 by RCA-I lectin pull-down assay. MCF-7ADR/shNC, MCF-7ADR/shB4GalT5, MCF-7ADR/NC, and MCF-7ADR/oe-B4GalT5 cells were lysed and incubated with agarose-bound RCA-I overnight. Total Frizzled-1 was used as loading control. All experiments were performed in three replicates. Data are presented as means±standard error of the mean. *$p < 0.05$, **$p < 0.01$ versus the control group.

ent with a feature of CSCs, namely a small subset of poorly differentiated tumor cells within a tumor. To further validate the relationship of B4GalT5 expression on the cell surface and BCSCs, we first constructed MCF-7ADR cells that stably overexpressed B4GalT5 with a C-terminal 6×His tag for immunofluorescence staining due to lack of the antibody recognizing its extracellular fragment (Fig. 4C). Western blotting analysis showed that ALDH1A1 was highly expressed in the B4GalT5-His–transfected cells, which suggested the successful construction of cells with active expression of B4GalT5-His (Fig. 4C). We then performed live cell staining using anti-His antibody. B4GalT5-His was detected in a small subset of cells by confocal microscopy without cell membrane permeabilization (Fig. 4D). Furthermore, fluorescence-activated cell sorting (FACS) analysis showed that cell surface B4GalT5-His was expressed in approximately 7.62% of MCF-7ADR cells (Fig. 4E and F). From these results, B4GalT5 was shown to partially localize to the cell membrane with its C-terminus extracellular region, and cell surface B4GalT5 still belonged to type II membrane-bound proteins, consistent with the normal localization of B4GalT5 on the Golgi apparatus [6].

Next, we explored the association between cell surface B4GalT5 and BCSCs by a series of *in vitro* assays. For convenient detection, we first detected the effect of B4GalT5 on CD44 expression by FACS analysis and observed that CD44 expression in MCF-7ADR cells was almost completely positive and not influenced by B4GalT5 overexpression (Fig. 4G and H). We then investigated the expression of CD24 and B4GalT5 on the cell surface of B4GalT5-His–expressing cells and found that the population with low and negative expression of CD24 ($CD44^{+}CD24^{-/low}$, BCSCs) accounted for 9.80% of the B4GalT5-His^{+} cells, whereas this population accounted for 26.10% of the B4GalT5-His^{-} cells (Fig. 4I). We also found that B4GalT5-His^{+} cells overlapped with not only $CD24^{+}$ cells but also $CD24^{-/low}$ cells, as observed by confocal microscopy analysis (Fig. 4J). These results suggested

that cell surface B4GalT5 may not be a marker of BCSCs. $ESA^+CD44^+CD24^{-/low}$ cells have also been reported to possess BCSC properties based on their high spheroid formation and *in vivo* tumor formation ability; hence, the molecular marker group is a more precise way to recognize BCSCs [2]. For further confirmation of the correlation of cell surface B4GalT5 and the stemness of BCSCs, the population rates of $ESA^+CD44^+CD24^{-/low}$ cells were detected in $CD44^+$ cells positive or negative for B4GalT5-His. As shown in Fig. 4K and L, FACS analysis demonstrated that the population with $ESA^+CD44^+CD24^{-/low}$ accounted for 10.93% of the B4GalT5-His^+ cells, while this population accounted for 20.57% of the B4GalT5-His^- cells, which was consistent with the results in Fig. 4H. Together, these results strongly suggest that there is no internal connection between cell surface B4GalT5 and BCSCs, and cell surface B4GalT5 is not responsible for the stemness of breast cancer.

5. B4GalT5 promotes Wnt/β-catenin signaling that is hyperactivated in BCSCs

Aberrant Wnt/β-catenin signaling is involved in multiple cancers and closely correlates with cell proliferation, invasion, metastasis, and CSC survival [16]. We tested whether Wnt/β-catenin signaling mediated the regulation of B4GalT5 on the stemness of BCSCs. To validate the relationship between Wnt/β-catenin signaling and BCSCs, we isolated $CD44^+CD24^{-/low}$ cells (BCSCs) and $CD44^+CD24^{-/low}$ cells (non-BCSCs) from MCF-7ADR cells using FACS, followed by immunofluorescence and western blotting analysis. GSK3β is reported to be phosphorylated at Ser 9 and thereby inactivated by AKT, resulting in a decrease in β-catenin degradation and activation of Wnt/β-catenin signaling [17]. We found that inactive phosphorylated-Gsk3β (Ser 9) is highly expressed in BCSCs (Fig. 5A). As the substrate of GSK3β, β-catenin showed low phosphorylation at Ser 45 and its expression was upregulated in BCSCs versus non-BCSCs, indicating that the stability of β-catenin was maintained in BCSCs (Fig. 5B and C). All these results suggest that Wnt/β-catenin signaling is hyperactivated in BCSCs compared with non-BCSCs.

To investigate the role of B4GalT5 in regulating Wnt/β-catenin signaling, we first depleted B4GalT5 using B4GalT5 siRNA in multiple breast cancer cell lines, including MCF-7ADR, MCF-7 and MDA-MB-231, and found that the expression levels of the Wnt/β-catenin signaling-related molecules Frizzled-1 and β-catenin were decreased significantly (Fig. 5D and E). In contrast, B4GalT5 overexpression significantly augmented the amounts of Frizzled-1 and β-catenin (Fig. 5F and G). As a canonical Wnt protein, wnt 3α is widely expressed and a representative ligand that interacts with the receptor Frizzled-1 and thereby activates the β-catenin–dependent pathway in Wnt signaling [18]. As shown in Fig. 5H and I, wnt 3α did not successfully induce activation of Wnt/β-catenin signaling and failed to reverse the decrease in stem cell marker ALDH1A1 expression in the B4GalT5-knockdown MCF-7ADR cells, further indicating that B4GalT5 regulates the stemness of breast cancer via activation of Wnt/β-catenin signaling.

We next elucidated the mechanisms underlying the decrease in β-catenin and Frizzled-1 induced by B4GalT5. While Wnt/β-catenin signaling is inactivated, the β-catenin destruction complex is formed and induces β-catenin phosphorylation and degradation by the proteasome system [18]. We observed that the proteasome inhibitor MG132 reversed the decrease in β-catenin in the B4GalT5-knockdown MCF-7ADR cells, whereas the amount of Frizzled-1 was not affected (Fig. 5J). In addition to the proteasomal pathway, the lysosomal system is the other major pathway for protein degradation, especially for cell surface receptors [19]. As the receptor of Wnt signaling, Frizzled-1 was found to be almost completely located on the cell membrane (Fig. 5K), and treatment with the lysosome inhibitor leupeptin clearly blocked B4GalT5 knockdown-induced downregulation of Frizzled-1 in MCF-7ADR cells (Fig. 5L). Together, these results indicate that B4GalT5 knockdown induces degradation of Frizzled-1 via the lysosomal pathway and thereby contributes to β-catenin degradation by the proteasomal pathway, which leads to inactivation of Wnt/β-catenin signaling.

Frizzled-1 is a receptor glycoprotein with N-glycosylation modification, as reported on the Uniprot website (http://www.uniprot.org). Glycans, which are bulky hydrophilic polymers, often contribute to increased stability against proteolysis. Moreover, the covalent binding of glycans to the protein surface may inherently enhance the thermal and kinetic stability of proteins [20]. B4GalT5 participates in the biosynthesis of N-linked oligosaccharides containing galactose residues [6]. Therefore, we assessed whether B4GalT5 participated in the N-glycosylation modification of Frizzled-1 and consequently affected Wnt/β-catenin signaling. RCA-I binds to galactose or N-acetylgalactosamine residues of membrane glycoconjugates, and RCA-I pull-down assays indicated that B4GalT5 knockdown significantly blocked the biosynthesis of galactosyl-oligosaccharides in the glycans of Frizzled-1, while B4GalT5 overexpression increased its biosynthesis (Fig. 5M), indicating a positive correlation between B4GalT5 and Frizzled-1 N-glycosylation. Above all, these findings strongly indicate that B4GalT5 promotes N-glycosylation of Frizzled-1 and its downstream signaling, thereby regulating the stemness of BCSCs.

Discussion

Increasing evidence suggests that BCSCs are involved in tumor progression, recurrence and resistance to chemo- and radiotherapies [3]; thus, identifying specific factors that can regulate BCSC properties is important for reducing recur-

rence and thereby improving the therapeutic effect on breast cancer. In this paper, we demonstrated that B4GalT5-mediated regulation of BCSCs positively correlated with malignant phenotypes and poor prognosis of breast cancer by a series of online database analyses and IHC analyses followed by *in vitro* and *vivo* studies.

A characteristic feature of the malignant transformation of tumor cells is the alteration of highly branched N-linked oligosaccharides on glycoproteins [4]. Abnormal expression of B4Gal-T1-T7 has been reported to be involved in changes in highly branched N-linked oligosaccharides, which are implicated in a number of diseases, including various cancers, inflammation, and viral infection [6]. For example, B4GalT2 is a critical effector involved in neuronal development, congenital muscular dystrophies and astrocytoma [21]. B4GalT4 overexpression is closely associated with colorectal cancer metastasis and poor prognosis in patients [22]. B4GalT5 and B4GalT6 are responsible for the production of lactosylceramide (LacCer) synthase, which functions in the initial step of ganglioside biosynthesis [23]. Moreover, B4GalT5 participates in the synthesis of both N-linked oligosaccharides and various glycolipids, contributing to highly galactosylated cell surface proteins that are associated with extraembryonic development and the tumorigenesis of astrocytoma, melanoma and glioma [6]. Finally, B4GalT7 regulates the synthesis of glycosaminoglycans that play a central role in many pathophysiological events [24]. In this paper, we found that the expression levels of B4GalTs (except B4GalT6) were upregulated in invasive breast carcinomas compared with mammary tissues, yet only B4GalT5 was found to be positively associated with the BCSC marker ALDH1A1, indicating that B4GalT5 displays CSC-related specificity and might play important roles in breast cancer.

Several studies have reported that Wnt/β-catenin signaling is aberrantly activated in various human malignancies, including breast, colorectal, gastric, lung, ovary, pancreatic, prostate and uterine cancers, leukemia and melanoma, and is involved in CSC survival, bulk tumor expansion and metastasis [25]. In this pathway, the Wnt ligand interacts with the receptor Frizzled-1, inhibiting the degradation of β-catenin and subsequently translocating into the cell nucleus, which can regulate the transcription of a number of target genes related to cancer development [25]. Our studies also confirmed that Wnt/β-catenin signaling was more active in BCSCs than in non-BCSCs. As the receptor of Wnt/β-catenin signaling, Frizzled-1 shows N-glycosylation that has been demonstrated to play an important role in regulating biological activity, intracellular targeting, protein folding, and maintenance of protein stability [26]. We propose for the first time that B4GalT5 mediates the biosynthesis of galactosyl-oligosaccharides in the N-glycosylation modification of Frizzled-1, which contributes to the activation of Wnt/β-catenin signaling and thereby regulates the stemness of breast cancer. Furthermore, we found that B4GalT4 knockdown promoted Frizzled-1 degradation by the lysosomal pathway and then contributed to the degradation of β-catenin through the proteasomal pathway. Previous studies have reported that incomplete N-glycosylation affects the stability of cell surface proteins, such as N-cadherin and programmed death-ligand 1, and leads to their ubiquitylation and subsequent proteasomal degradation [27,28], which is inconsistent with our findings. Since proteins on the cell membrane recycle from endosomes to the plasma membrane or are transported to lysosomes for degradation [29], we believe that incomplete N-glycosylation resulting from the depletion of B4GalT5 affects the stability of Frizzled-1 located in the cell membrane and eventually results in its degradation through the lysosomal pathway.

In addition to the location of B4GalTs in the Golgi complex, glycosyltransferases are present on the cell surface, where they function as adhesion molecules that are involved in cell-to-cell and cell-to-extracellular matrix interactions as well as cell spreading and migration, and associated with signal transduction cascades [15,30]. Consistent with these previous studies, our data also showed that B4GalT5 was located on the cell surface of MCF-7ADR cells and first confirmed that it is a type II membrane-bound protein. As B4GalT5, located partly on the cell surface, was related to cell spreading and migration [15], cell surface B4GalT5 may be a molecular marker for the stemness of BCSCs. However, flow cytometry and immunofluorescence assays revealed that cell surface B4GalT5 was not responsible for the stemness of BCSC. These results in turn demonstrated that B4GalT5 canonically located in the Golgi complex, which affected the level of Frizzled-1 by glycosylation modification on the cell surface, was responsible for the stemness of breast cancer through Wnt/β-catenin signaling. The biological function of cell surface B4GalT5 may only mediate spreading and migration of a small number of cells. The finding of a correlation between glycosyltransferase distribution and its function in BCSCs provides more foundations for drug design to target BCBCs.

In conclusion, we showed that B4GalT5 is overexpressed in invasive breast carcinomas, positively associated with poor survival, and closely related to the stemness of BCSCs. We have demonstrated for the first time that B4GalT5 regulates BCSC properties by affecting the N-glycosylation modification of Frizzled-1, thereby affecting its stability on the cell membrane and inhibiting downstream signaling in BCSCs, which is independent of the B4GalT5 location in cells. Our findings provide novel insights into the important role of B4GalT5 in BCSCs. This study also suggests that targeting B4GalT5 may be a promising strategy to suppress or eliminate CSCs in breast cancer.

Electronic Supplementary Material

Supplementary materials are available at Cancer Research and Treatment website (https://www.e-crt.org).

Conflicts of Interest

Conflicts of interest relevant to this article was not reported.

Acknowledgments

This work was supported by the National Natural Science Foundation of China [No. 81673450] and the NSFC Shandong Joint Fund [U1606403]; the Scientific and Technological Innovation Project was financially supported by Qingdao National Laboratory for Marine Science and Technology [No. 2015ASKJ02], the Fundamental Research Funds for the Central Universities [No. 201762002] and the National Science and Technology Major Project for Significant New Drugs Development (2018ZX09735-004).

References

1. Bray F, Ferlay J, Soerjomataram I, Siegel RL, Torre LA, Jemal A. Global cancer statistics 2018: GLOBOCAN estimates of incidence and mortality worldwide for 36 cancers in 185 countries. CA Cancer J Clin. 2018;68:394-424.
2. Visvader JE, Lindeman GJ. Cancer stem cells: current status and evolving complexities. Cell Stem Cell. 2012;10:717-28.
3. Ghasemi F, Sarabi PZ, Athari SS, Esmaeilzadeh A. Therapeutics strategies against cancer stem cell in breast cancer. Int J Biochem Cell Biol. 2019;109:76-81.
4. Fuster MM, Esko JD. The sweet and sour of cancer: glycans as novel therapeutic targets. Nat Rev Cancer. 2005;5:526-42.
5. Pinho SS, Reis CA. Glycosylation in cancer: mechanisms and clinical implications. Nat Rev Cancer. 2015;15:540-55.
6. Wassler M. β1,4-galactosyltransferases, potential modifiers of stem cell pluripotency and differentiation. In: Bhartiya D, Lenka, N, editors. Pluripotent stem cells. Rijeka: InTech; 2013. p. 345-72.
7. Ma Y, Zhang P, Wang F, Yang J, Yang Z, Qin H. The relationship between early embryo development and tumourigenesis. J Cell Mol Med. 2010;14:2697-701.
8. Gyorffy B, Lanczky A, Eklund AC, Denkert C, Budczies J, Li Q, et al. An online survival analysis tool to rapidly assess the effect of 22,277 genes on breast cancer prognosis using microarray data of 1,809 patients. Breast Cancer Res Treat. 2010;123:725-31.
9. Tang Z, Li C, Kang B, Gao G, Li C, Zhang Z. GEPIA: a web server for cancer and normal gene expression profiling and interactive analyses. Nucleic Acids Res. 2017;45:W98-W102.
10. Muller A, Homey B, Soto H, Ge N, Catron D, Buchanan ME, et al. Involvement of chemokine receptors in breast cancer metastasis. Nature. 2001;410:50-6.
11. Robey RW, Pluchino KM, Hall MD, Fojo AT, Bates SE, Gottesman MM. Revisiting the role of ABC transporters in multidrug-resistant cancer. Nat Rev Cancer. 2018;18:452-64.
12. Ciccone V, Terzuoli E, Donnini S, Giachetti A, Morbidelli L, Ziche M. Stemness marker ALDH1A1 promotes tumor angiogenesis via retinoic acid/HIF-1alpha/VEGF signalling in MCF-7 breast cancer cells. J Exp Clin Cancer Res. 2018;37:311.
13. Li Y, Xian M, Yang B, Ying M, He Q. Inhibition of KLF4 by statins reverses adriamycin-induced metastasis and cancer stemness in osteosarcoma cells. Stem Cell Reports. 2017;8:1617-29.
14. Yang A, Qin S, Schulte BA, Ethier SP, Tew KD, Wang GY. MYC inhibition depletes cancer stem-like cells in triple-negative breast cancer. Cancer Res. 2017;77:6641-50.
15. Youakim A, Dubois DH, Shur BD. Localization of the long form of beta-1,4-galactosyltransferase to the plasma membrane and Golgi complex of 3T3 and F9 cells by immunofluorescence confocal microscopy. Proc Natl Acad Sci U S A. 1994;91:10913-7.
16. Lim SK, Lu SY, Kang SA, Tan HJ, Li Z, Adrian Wee ZN, et al. Wnt signaling promotes breast cancer by blocking ITCH-mediated degradation of YAP/TAZ transcriptional coactivator WBP2. Cancer Res. 2016;76:6278-89.
17. Chung J, Karkhanis V, Baiocchi RA, Sif S. Protein arginine methyltransferase 5 (PRMT5) promotes survival of lymphoma cells via activation of WNT/beta-catenin and AKT/GSK3beta proliferative signaling. J Biol Chem. 2019;294:7692-710.
18. Rada P, Rojo AI, Offergeld A, Feng GJ, Velasco-Martin JP, Gonzalez-Sancho JM, et al. WNT-3A regulates an Axin1/NRF2 complex that regulates antioxidant metabolism in hepatocytes. Antioxid Redox Signal. 2015;22:555-71.
19. Cooper GM. The cell: a molecular approach. 2nd ed. Sunderland, MA: Sinauer Associates Inc.; 2000.
20. Sola RJ, Griebenow K. Effects of glycosylation on the stability of protein pharmaceuticals. J Pharm Sci. 2009;98:1223-45.
21. Sasaki N, Manya H, Okubo R, Kobayashi K, Ishida H, Toda T, et al. beta4GalT-II is a key regulator of glycosylation of the proteins involved in neuronal development. Biochem Biophys Res Commun. 2005;333:131-7.
22. Chen WS, Chang HY, Li CP, Liu JM, Huang TS. Tumor beta-1,4-galactosyltransferase IV overexpression is closely associated with colorectal cancer metastasis and poor prognosis. Clin Cancer Res. 2005;11(24 Pt 1):8615-22.
23. Yoshihara T, Satake H, Nishie T, Okino N, Hatta T, Otani H, et al. Lactosylceramide synthases encoded by B4galt5 and 6 genes are pivotal for neuronal generation and myelin formation in mice. PLoS Genet. 2018;14:e1007545.
24. Talhaoui I, Bui C, Oriol R, Mulliert G, Gulberti S, Netter P, et al. Identification of key functional residues in the active site of human {beta}1,4-galactosyltransferase 7: a major enzyme in the glycosaminoglycan synthesis pathway. J Biol Chem. 2010;285:37342-58.
25. Katoh M. Canonical and non-canonical WNT signaling in cancer stem cells and their niches: cellular heterogeneity, omics reprogramming, targeted therapy and tumor plasticity

(Review). Int J Oncol. 2017;51:1357-69.
26. Wang H, Zhou T, Peng J, Xu P, Dong N, Chen S, et al. Distinct roles of N-glycosylation at different sites of corin in cell membrane targeting and ectodomain shedding. J Biol Chem. 2015;290:1654-63.
27. Li CW, Lim SO, Xia W, Lee HH, Chan LC, Kuo CW, et al. Glycosylation and stabilization of programmed death ligand-1 suppresses T-cell activity. Nat Commun. 2016;7:12632.
28. Xu Y, Chang R, Xu F, Gao Y, Yang F, Wang C, et al. N-glycosylation at Asn 402 stabilizes N-cadherin and promotes cell-cell adhesion of glioma cells. J Cell Biochem. 2017;118:1423-31.
29. Yonamine I, Bamba T, Nirala NK, Jesmin N, Kosakowska-Cholody T, Nagashima K, et al. Sphingosine kinases and their metabolites modulate endolysosomal trafficking in photoreceptors. J Cell Biol. 2011;192:557-67.
30. Rodeheffer C, Shur BD. Targeted mutations in beta1,4-galactosyltransferase I reveal its multiple cellular functions. Biochim Biophys Acta. 2002;1573:258-70.